Desalination and Water Treatment
www.deswater.com

doi: 10.5004/dwt.2019.23634

146 (2019) 165–175
April

In-situ sludge reduction and simultaneous phosphorus removal in A^2O and side-stream induced crystallization coupling system for treating domestic wastewater

Yonglei Wang[a,b,c,*], Baozhen Liu[a], Kefeng Zhang[a], Yongjian Liu[d], Xuexin Xu[a], Hongbo Wang[a,*]

[a]*College of Environmental and Municipal Engineering, Shandong Jianzhu University, 250101, Jinan, China, emails: wyl1016@sdjzu.edu.cn (Y. Wang), wanghongbo@sdjzu.edu.cn (H. Wang), liubaozhen_119@163.com (B. Liu), kfz@sdjzu.edu.cn (K. Zhang), 997434882@qq.com (X. Xu)*
[b]*Shandong Province City Water Supply and Drainage Water Quality Monitoring Center, 250021, Jinan, China*
[c]*College of Environment Science and Engineering, Tongji University, 200092, Shanghai, People's Republic of China*
[d]*Shandong Huaihe River Basin Water Conservancy Administration Planning and Design Institute, 250014, Jinan, People's Republic of China, email: 95387013@qq.com*

Received 2 July 2018; Accepted 11 December 2018

ABSTRACT

Biofilm in-situ sludge reduction process can reduce the yield of excess sludge and restrict biological phosphorus removal efficiency. In this study, a novel in-situ sludge reduction coupled side-stream induced crystallizing (SIC) phosphorus removal process was proposed. The feasibility of simultaneous high efficiency in-situ sludge reduction and removal of nutrients from domestic sewage, and SIC phosphorus removal potential were investigated. The results showed that operation effect of A^2O–SIC was excellent with anaerobic supernatant side-stream flow ratio 40%, and pH 8, reaction time 30 min, seed size 100–150 mesh, aeration volume 300 L/h, Ca/P ratio 2.5, and seed dosage of 50% in SIC. The Y_{obs} of A^2O–SIC was 0.18±0.05 g MLSS/g COD reducing 18.18% excess sludge than A^2O sludge reduction process. The average concentration of effluent TP was 0.54 mg·L^{-1}, and the removal rate was 88.89%. SIC does not affect the microbial activity of the biological system, whereas Ca^{2+} in the reflux liquid can promote the production of extracellular polymer and consequently, the formation of biofilm. Energy dispersive spectrometer test found that the proportion of P element on the seed crystal surface was significantly increased. In addition, the anaerobic area dominant species were *Thauera, Methyloversatilis* in the A^2O–SIC and biological phosphorus removal was not inhibited. The experimental results provide an effective solution for simultaneous high-efficiency in-situ sludge reduction and phosphorus removal in wastewater treatment.

Keywords: A/A/O; In-situ sludge reduction; Lateral flow system; Induced crystallizing phosphorus removal; Hydroxyapatite (HAP)

1. Introduction

Nowadays, excessive P loads to water bodies from industrial, agricultural, and household wastes may cause serious eutrophication [1]. Therefore, stringent effluent quality standards for wastewater treatment plants (WWTPs) are compulsively implemented by many national governments of the world. In China, P concentration from WWTPs should meet the strict discharge limit of less than 0.5 mg/L [2]. Biological phosphorus removal method is widely used as the most economical and environmentally friendly method in the WWTPs. Phosphate accumulating organisms (PAOs) is of fundamental importance to P removal in biological process. Based on PAOs metabolism mechanism, at anaerobic phase, PAOs

* Corresponding authors.

could release P into the liquid and then, in the subsequent anoxic phase, uptake P in excess into the cell in the form of poly-P and finally, discharge of excess P-rich activated sludge to achieve P removal [3,4]. However, it can increase the production of excess sludge from WWTPs, which is an economic burden restricting the running of sewage treatment plants [5,6]. Yan et al. [7] studied the sludge reduction and recover phosphorus simultaneously, and found that the low excess sludge discharge directly leads to low biological phosphorus removal efficiency [8]. The contradiction between in-situ sludge reduction process and biological phosphorus removal is one of the significant issues that restrict the development of application and promotion of in-situ sludge reduction process. Research a process that can simultaneously reduce excess sludge and remove phosphorus is the development direction of the sludge reduction process.

In addition, as a non-renewable resource, phosphorus can also reduce the phosphorus content in the effluent via collecting and recycling from phosphorus-containing domestic sewage. Theoretical calculations showed that approximate 15%–20% of total global phosphate demand could be satisfied by recovering the P from real domestic sewage [9].The lysis and digestion by anaerobic digestion in the in-situ sludge reduction process can provide P-rich supernatants, making it possible to use phosphorus reuse processes in combination with in-situ sludge reduction processes to achieve P removal. A variety of processes have been developed to assist in the efficient removal and recovery of P in wastewater [10,11]. Induced crystallization is chemical method for removing phosphorus from solution. Compared with other chemical methods, the crystalline product has low moisture content and can be easily separated and reused [1,3]. Hydroxyapatite (HAP, $Ca_5(PO_4)_3OH$) and struvite (magnesium ammonium phosphate [MAP] $MgNH_4PO_4$) are two commonly used inductive crystallization techniques. Compared with MAP, HAP can be used to recover phosphorus from wastewater containing low concentration of phosphorus, especially the in-situ sludge reduction process. The use of side-stream combined with HAP removal P has broad application prospects [12,13]. However, it is unclear whether side-stream inducing crystallizing phosphorus removal will affect the sludge reduction effect via biofilm in-situ sludge reduction process and the removal of COD, N and P in mainstream biological system. The influence of side-stream induced crystallizing (SIC) on the activity of PAOs in biofilm systems also needs further exploration.

In this study, a novel process of sludge in-situ reduction and side-stream induced crystallization coupling system, called A^{2}O-SIC, was proposed for simultaneous removal of COD, N, P and minimal sludge production and then, preparation for phosphorus recovery. The specific objectives were: (1) to assess the efficiency of SIC under different operating conditions (seed particle size, filling ratio, Ca/P ratio, and side flow ratio) and the effect on A^{2}O biofilm in-situ sludge reduction system; (2) to investigate the effect and coupling mechanism of SIC on A^{2}O in-situ sludge reduction process; (3) to analyze the effect of SIC on biological population of A^{2}O biofilm in-situ sludge reduction process. The results obtained here could be beneficial to development of a combined process for simultaneous in-situ sludge reduction and efficient removal of pollutants and phosphorus from domestic sewage.

2. Materials and methods

2.1. Experimental set-up

In this study, a lab-scale A^{2}O-SIC system (Fig. 1) consisting of two reactors made from polymethyl methacrylate, that is, one for the A^{2}O process (anaerobic/anoxic/aerobic) and the other for the SIC was used in a phosphorus removal column. The working volume of the A^{2}O process was 144 L (the volumes of anaerobic, anoxic, and aerobic were 32, 32, and 80 L, respectively). And that of the SIC process was 10 L, with two zones, for crystallization reaction and settling. The A^{2}O was inoculated with active sludge from a full-scale WWTP (A^{2}O process) located in Jinan, China. The operation condition for A^{2}O and A^{2}O-SIC lasted approximately 400 d. During the test, floating spherical carriers (FSCs) with a compound of polyurethane and two fiber balls formed a biofilm, which was were required to enhance the endogenous respiration of the biomass and for metabolic uncoupling. This greatly reduced the excess sludge production. The SIC operation started on

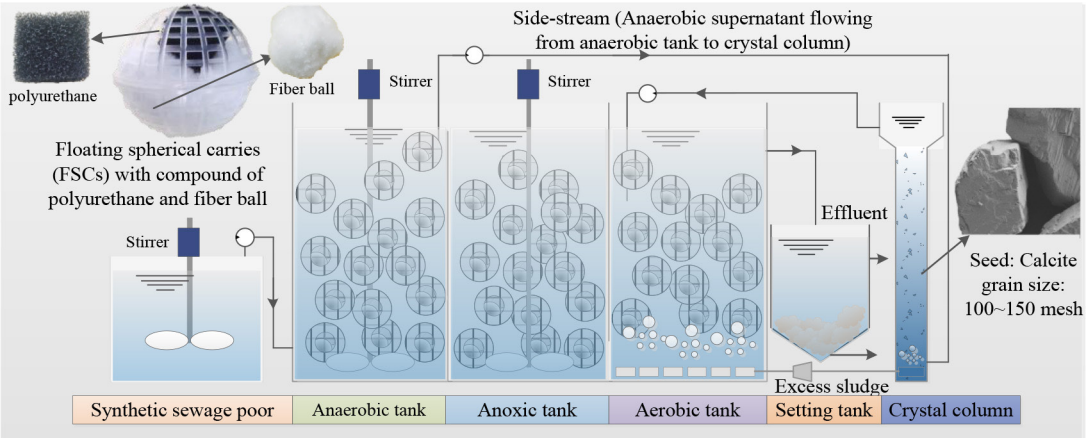

Fig. 1. Schematic diagram of experimental set-up. Mainstream direction: synthetic sewage pool, and the anaerobic, anoxic, aerobic, and setting tanks; Lateral flow direction: from anaerobic supernatant mixed with calcium chloride to the crystallization reaction zone, supernatant in crystal column settling area returns to the aerobic tank.

the 225th day, and calcite was filled in the column as the seed. The anaerobic tank supernatant flowed into the crystallization column sideways, and then the upper settling supernatant flowed from crystallization column back to the aerobic tank. Finally, the effluent was discharged as an overflow through the sedimentation tank and the excess sludge was returned to the anaerobic tank from the bottom of the sedimentation tank. The hydraulic retention time (HRT) was set to 12 h, and the HRT for the anaerobic, anoxic and aerobic were set to 2.67, 2.67 and 6.67 h, respectively. The A^{2}O and A^{2}O-SIC were operated at room temperatures ranging from 20°C to 25°C. The mixed liquor suspended solids (MLSS) was maintained at approximately 4,000 mg/L, and the solids retention time was set to 10 d. The synthetic wastewater used in this study included 510 mg/L, $MgSO_4$ at 90 mg/L, 14 mg/L $CaCl_2$, NH_4Cl at 153 mg·L^{-1}, Na_2HPO_4 at 46 mg·L^{-1}, yeast extract at 10 mg/L, and 0.3 mL/L of a trace elements solution prepared according to Smolders et al. [14]. The pH was maintained between 6.9 and 7.5 by the addition of Na_2CO_3. The detailed composition of synthetic wastewater follows: COD, 250–380 mg·L^{-1}; NH_4^+-N, 40–50 mg·L^{-1}; total phosphorus (TP), 10–15 mg·L^{-1}.

2.2. Experimental design

To investigate the optimal operation conditions of SIC and examine the P removal performance, the particle size of the calcite, seed filling ratio and Ca/P molar ratio were gradually increased from 60 to 80, 100 to 150, and 200 to 250 mesh; 30%, 50%, 70%, and 80%; and 1.5, 2.0, 2.5, 3.0, and 3.5, respectively. To assess whether and how P removal influences the A^{2}O-SIC performance, the side-stream ratios, representing the flow ratio from anaerobic supernatant to SIC to influent were gradually increased from 0% to 30%, 40% and 45% to examine the P removal performance. Each phase was run for 30 d. In the induced HAP crystallization, the $CaCl_2$ solution was used to provide the appropriate Ca/P molar ratio in solution. In the SIC, air was supplied at the flow rate of 300 L/h to strip carbon dioxide from the solution, thus enhancing its pH value of solution to over 8.5.

2.3. Analytical methods

COD, NH_4^+-N, TN, and TP were measured by dichromate titration, Nessler's reagent spectrophotometry, the ammonium molybdate spectrophotometric method, ultraviolet spectrophotometry, respectively, and the MLSS were measured in fresh samples using quantitative filter paper by gravimetric method (Chinese NEPA). Dissolved oxygen (DO), pH, and ORP values were monitored by portable DO, pH, and ORP meters (HACH, USA), respectively. The biofilm samples under steady state were extracted by the ultrasonic method from the FSC according to Zhang et al. [15]. Then, samples were then used to analyze the microbial activity, EPS, microbial community and SEM of the biofilm during the A^{2}O and A^{2}O-SIC operations. A modified heat extraction method was used to extract EPS [16,17]. The protein (PN) and polysaccharide (PS) content in the EPS was determined by the Lowry and phenol–sulfuric acid methods. The Lowry method used the protein assay kit (Shanghai LAB-AIDE Co., Ltd., China), with bovine serum albumin as the standard, and the phenol-sulfuric acid method used glucose as the standard. The pretreatment of SEM samples in different zones was measured according to Text S1 in the supplementary information. The microbial communities of A^{2}O-SIC were analyzed by high-throughput sequencing, and the specific operational steps of DNA extraction, PCR amplification, and high-throughput 454 pyrosequencing were carried out according to Text S2 in the supplementary information [17]. The sludge sample dyeing method was based on Zhang et al. [18]. The formulas of accumulation (Y_{obs}) and accumulation ratio of excess sludge values were according to Wang et al. [19], and the detail was in section 3 of supplementary information.

3. Results and discussion

3.1. Effects of the side-stream induced crystallization process

3.1.1. Effect of seed particle size

It can be seen from Fig. 2(a) that the grain size of the seed crystal gradually increased, and the phosphorus removal effect of the induced crystal gradually increased and then decreased rapidly. The effect of removing phosphorus from 100 to 150 mesh particle size was the best. The removal rate was over 89% and the highest removal rate was 91.12%. The seed crystals mainly provide carriers for HAP crystallization to promote the formation of crystal nucleus [20]. Seckler et al. [21] found that grain size affects the liquid-phase flow state, frictional strength, and crystal adhesion properties. The experimental results were similar to Song et al. [22], when the particle size of calcite was changed from 60–80 mesh to 200–250 mesh, the phosphorus removal efficiency of the crystalline column increased from 66.92% to 89.0% and then decreased to 80.23%. HAP crystals need to be formed under alkaline conditions [1]. Small grain size can deposit on the bottom of the crystallizer to form a fixed bed, affecting the reactor fluidized mixed state and phosphorus removal. Crystalline is a kind of microcrystal fine particle morphology [12]. Oversized grain affected the crystal deposition on the seed crystal, and the effect of phosphorus removal was reduced. In addition, suitable grain size under aeration can greatly form fluidization, favoring the induced HAP crystallization reaction.

3.1.2. Effect of seed dosage

The seeding dosage gradually increased from 30% to 80%, and the phosphorus removal rate increased from 46.3% to 90.01% and gradually decreased to 78.26% (Fig. 2(b)). This result was similar to Tervahauta et al. [23]. Calcite can make the crystal ions in the solution gather in the local region, increased the concentration product of the crystal ions, and induced the crystallization [22]. The number of seed crystals can affect the probability of localized crystal ion aggregation and local concentration in the solution. The increase of the seed content can increase the seed surface area in the phosphorus removal column, provide a larger attachment surface for the crystal, and improve the probability of increasing the local concentration of the constitutional crystal ions. However, an excessively high seeding ratio increased the density of seed crystals in the crystal column. High-density seed crystals formed a fluidized state under aeration, and

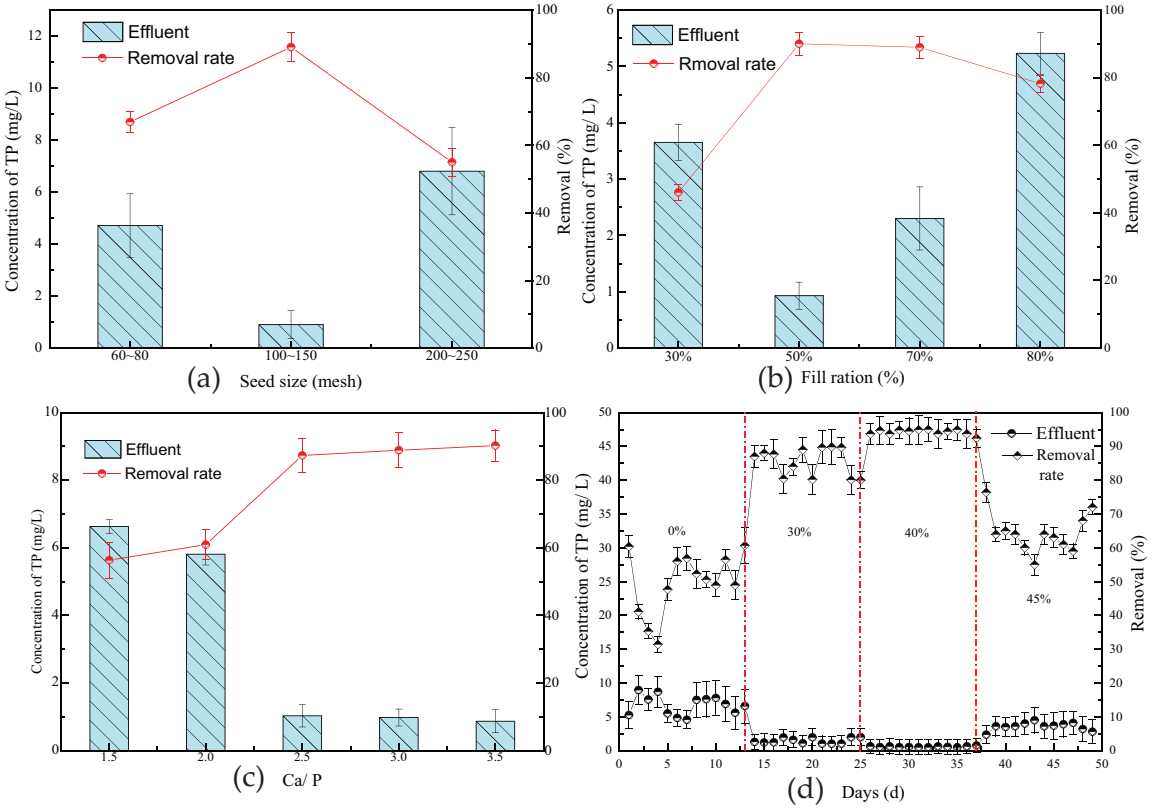

Fig. 2. Effects of the side-stream induced crystallization process seed size (a), fill ratio (b), Ca/P (c), and lateral flow ratios (d).

the friction between particles increased accordingly. This phenomenon can destroy the crystal structure formed on the seed surface and reduce the phosphorus removal rate.

3.1.3. Effect of Ca/P molar ratio

As can be seen from Fig. 2(c), when Ca/P was raised from 2.0 to 3.0, the phosphorus removal rate increased from 41.92% to 85.85%, increasing 42.93%. However, continued to increase the Ca/P ratio, the phosphorus removal rate was 90.23%, with little change. Ca^{2+} is one of the constitutional ions. Increasing the Ca^{2+} concentration is equivalent to increasing the concentration product of the constitutional crystal ions in the solution and, increasing the supersaturation of the crystallization system in the liquid phase. Therefore, the crystallization reaction proceeded in a positive direction [23,24]. When the Ca/P ratio is 2.0, the phosphorus removal rate was low, and the requirement of greater than Ksp = 55.67 cannot be satisfied. The constitutional crystal ions in the liquid phase are insufficient to react to form HAP crystals. However, the Ca/P ratio is greater than 3.0, the phosphorus removal rate is 90.23%, and the increase removal was not significant. In addition, increased the concentration of Ca^{2+} in the A^2O had a potential impact on the quality of the effluent.

3.1.4. Effect of side-stream ratio of anaerobic supernatant

The proportion of side-stream has a significant effect on the effluent phosphorus concentration. Fig. 2(d) shows that as the proportion of lateral flow increases from 0% to 40%, the effect of phosphorus removal increased and the effluent P concentration decreased from 6.72 to 0.50 mg·L^{-1}, reaching the emission standards. This indicates that side-stream induced crystallization in the A^2O-SIC process significantly increased the efficiency of biological phosphorus removal. This was mainly due to the reduction of phosphorus loading in mainstream systems. However, when the proportion of side-stream continued to rise to 45%, the accumulation of phosphorus removal deteriorated, and the effluent phosphorus concentration exceeded the standard, increasing from 0.50 to 3.57 mg·L^{-1}. The probable reason was that the excessively high proportion of side-stream leaded to large concentration Ca^{2+} entering into A^2O and inhibiting the metabolic activity of polyphosphate bacteria. Zhang et al. [25] found that the metabolic pathway of polyphosphates in the system changed with the increase of Ca^{2+}. The study of Zou et al. [26] also had similar conclusions, as the concentration of Ca^{2+} increased, the intracellular poly-P concentration decreased. In this study, the optimum operating conditions for the SIC were 40% of the anaerobic tank side flow ratio, pH at 8 and 30 min of continuous reaction time, using 100 to 150 mesh particle size seeds, the Ca/P molar ratio of 2.5 and the proportion of 50% seed crystal.

3.2. Performance and sludge yields of the A^2O and A^2O-SIC coupling systems

To further evaluate the efficiency and operational stability of A^2O-SIC process, the excess sludge yield, nutrient and phosphorus removal performance were tested under the optimal operating conditions. The experiment lasted for

400 d. Figs. 3 and 4 show the variety of excess sludge production and effluent COD, TP, NH_4^+-N, and TN, respectively. Fig. 3 shows that the Y_{obs} of A²O-SIC was 0.18±0.05 g MLSS/g COD, and accumulation and accumulation ratio of excess sludge values were 5.81 g MLSS/L and 0.031 g MLSS/(L·d), respectively. Compared with A²O in-situ sludge reduction process (Y_{obs}, accumulation and accumulation ratio of excess sludge values were 0.22±0.05 g MLSS/g COD, 8.42 g MLSS/L, and 0.037 g MLSS/(L·d), respectively), the A²O-SIC reduced sludge by 18.18% and the cumulative rate of excess sludge decreased by 16.22%. The SIC promoted the sludge reduction efficiency and maintain a good in-situ sludge reduction effect.

Fig. 4 shows that A²O-SIC had a good effect of simultaneous nitrogen and phosphorus removal with running stably for a long time. The average COD, TN, NH_4^+-N, and TP concentration of A²O-SIC effluent were 18.78, 11.18, 3.97, and 0.54 mg·L^{-1}, respectively. The average removal rate of COD, TN, NH_4^+-N, and TP were 90.36%, 67.73%, 93.18%, and

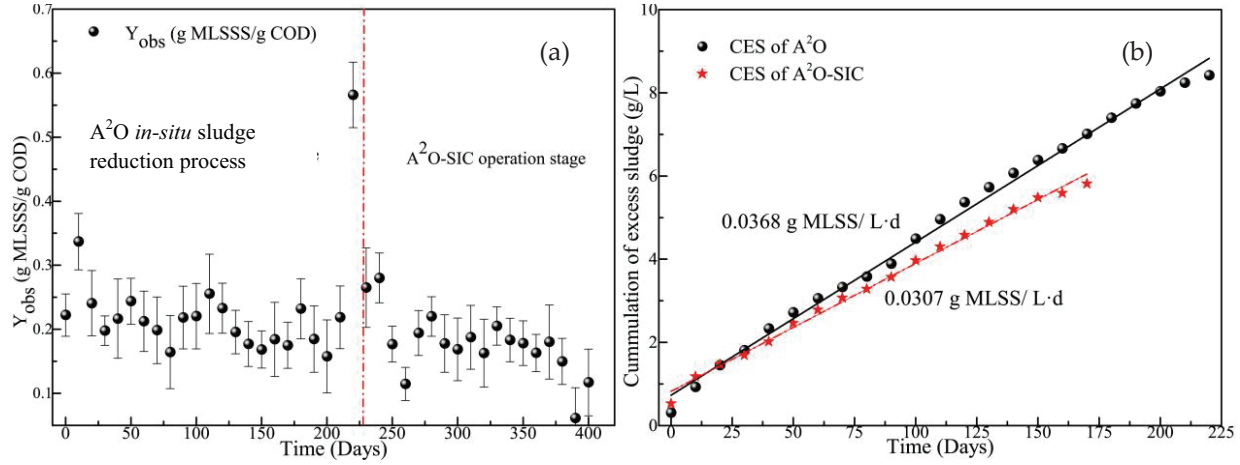

Fig. 3. Variations of Y_{obs} (a) and accumulation of excess sludge (b) during the experiment over 400 d.

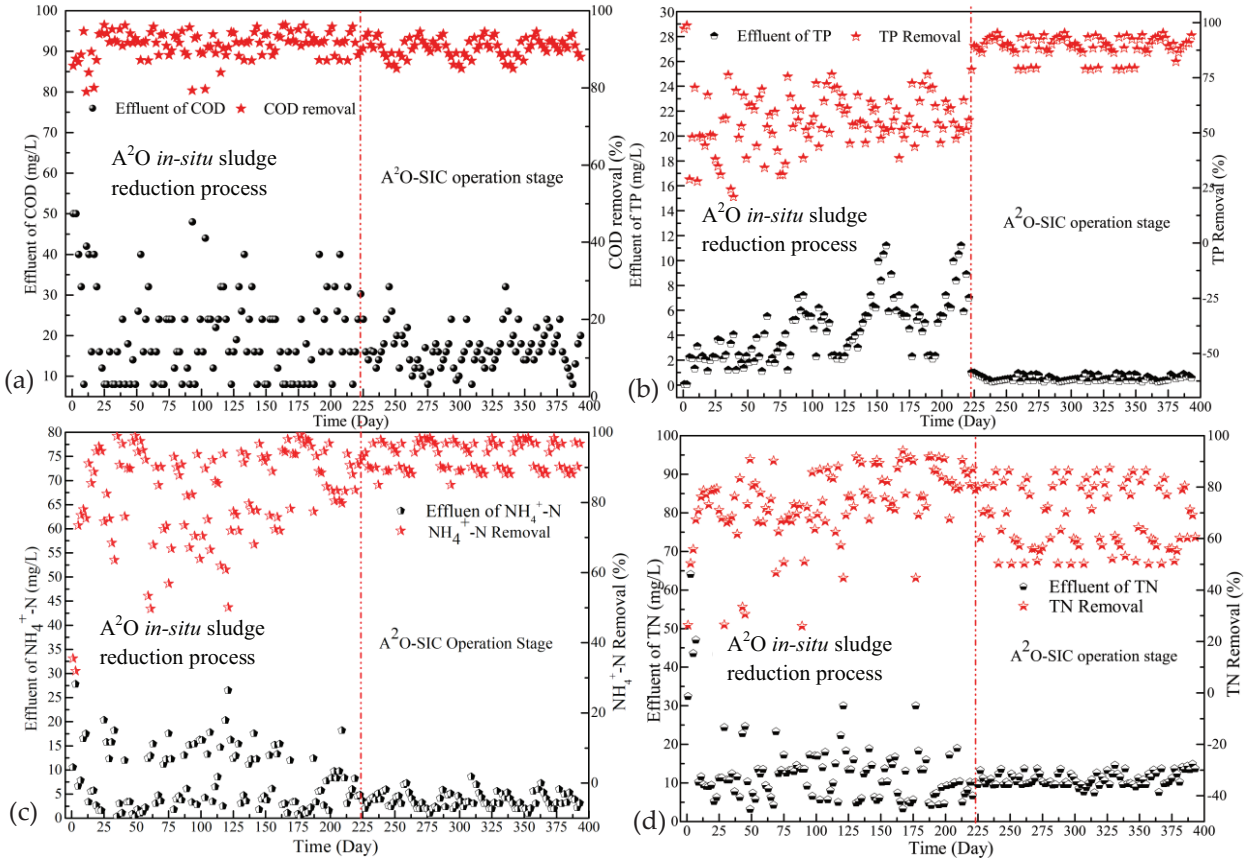

Fig. 4. Variations of COD (a), TP (b), NH_4^+-N (c), and TN (d) during the experiment over 400 d.

88.89%, respectively. Compared with the A²O in-situ sludge reduction process, the removal rate was improved, and the effluent water quality tends to be stable. The average concentration of effluent TP can maintain the national control standard of 0.5 mg·L^{-1}.

3.3. Coupling mechanism of the A²O-SIC combined process

In order to further study the coupling effect between the SIC and A²O, the change of EPS concentration in the supernatant of the biological system before and after the SIC running and the nutrients change of anaerobic/SIC/effluent along the flow direction of the A²O-SIC were detected. As shown in Fig. 5, the content of polysaccharide and protein in the A²O-SIC supernatant was increased compared with the A²O in-situ reduction process, and the EPS content was increased from 146.14 mg/mg VSS to 594.12 mg/mg VSS. The Ca^{2+}-rich reflux was led into the A²O inducing secreted EPS according to Sheng et al. [27]. EPS is an important factor influencing the formation of biofilm. High concentration of EPS can promote the formation of biofilm, increase the mutual adhesion of microorganisms, and reduce the excess sludge. As shown in Table 1, the SIC unit can only effectively remove phosphorus with no removal effect on COD, NH_4^+-N, and TN. Similar to the study of Wu et al. [28], the nutrients-rich reflux was led into the aerobic area providing supplemental carbon source, which can improve organic concentration and promote heterotrophic microbial activity at the end of the system. As above analysis, the SIC can increase phosphorus removal rate of A²O-SIC process, promote sludge in-situ reduction and increase pollutant removal rate. Therefore, SIC effectively couple with mainstream process.

3.4. SEM micrographs and energy dispersive spectrometer (EDS) analysis graph

The morphology of crystallites and crystals was observed by SEM, and the composition of crystal elements on the surface of seeds was quantitatively analyzed by EDS. SEM micrographs of seeds and microcrystalline in SIC are shown in Figs. 6(a) and (b). The surface of calcite has a smooth surface (Fig. 6(a)), and then the seed became rough after a period of reaction (Fig. 6(b)). The granular substances overlap and adhere to the surface of the seed, and the irregularly distributed crystal morphology was presumed to be the HAP, which was similar to the study of Dai et al. [1] and Seckler et al. [21]. From the EDS analysis graph (Figs. 6(c) and (d)), the proportion of P on seed surface was obviously increased. This indicated that the surface of the seed crystal adhered to the phosphorus-rich crystal, which was speculated to be HAP crystal. However, the proportion of carbon also rose after crystallization inducing $CaCO_3$ sediment was easily formed on the surface of seed.

3.5. Characteristics of the microbial community in the A²O-SIC

3.5.1. Analysis of biofilm microbial polymer

To further analyze the effect of SIC on the PAOs in the A²O-SIC, the sludge sample on biofilm was carried out using staining observation. As shown in Fig. 7(a), filamentous bacteria, bacilli, and large cocci contain black PHB(poly-β-hydroxybutyrate) particles, and microorganism and bacillus on the biofilm contain black poly-P in the aerobic area (Fig. 7(b)). In the A²O process, the main forms of PAOs on the

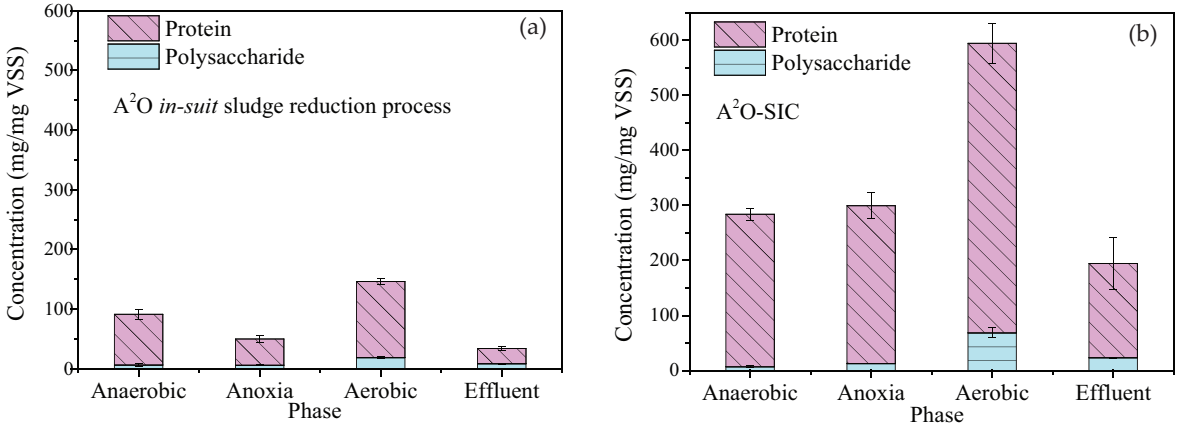

Fig. 5. Variations in EPS in different phases of A²O (a) and A²O-SIC (b).

Table 1
Changes of nutrient concentration along the water flow

Phase	COD (mg/L)	NH_4^+-N (mg/L)	TN (mg/L)	TP (mg/L)
Anaerobic	110.23±22.35	60.55±3.56	61.32±4.88	12.56±2.69
SIC	109.45±11.87	56.14±2.39	57.48±3.28	2.98±2.92
SIC removal (%)	0.71±0.023	7.28±1.54	6.26±3.41	72.07±23.58
Effluent	18.14±12.54	3.76±2.48	9.33±7.31	1.10±0.21
Removal (%)	90.66%±6.65	90.43±4.16	75.69±12.50	84.06±4.52

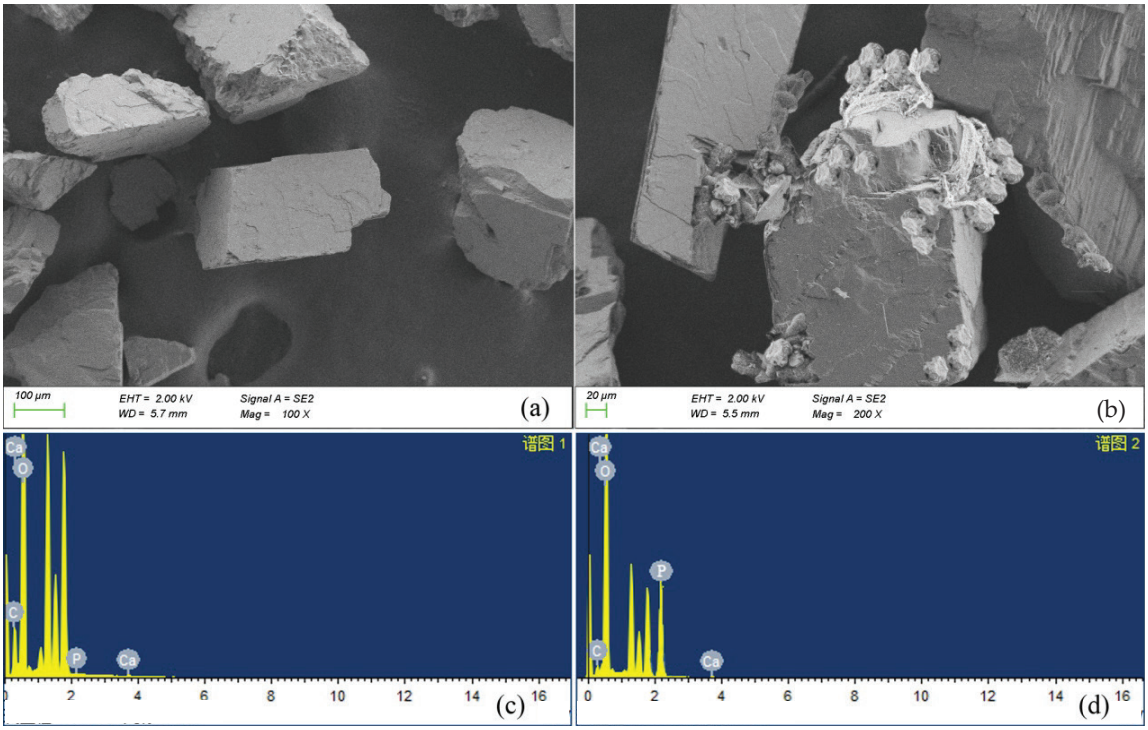

Fig. 6. SEM micrographs and EDS analysis graphs of seeds and microcrystalline structures in SIC. SEM image of (a) seeds and (b) microcrystalline; EDS analysis graph of (c) seeds and (d) microcrystalline.

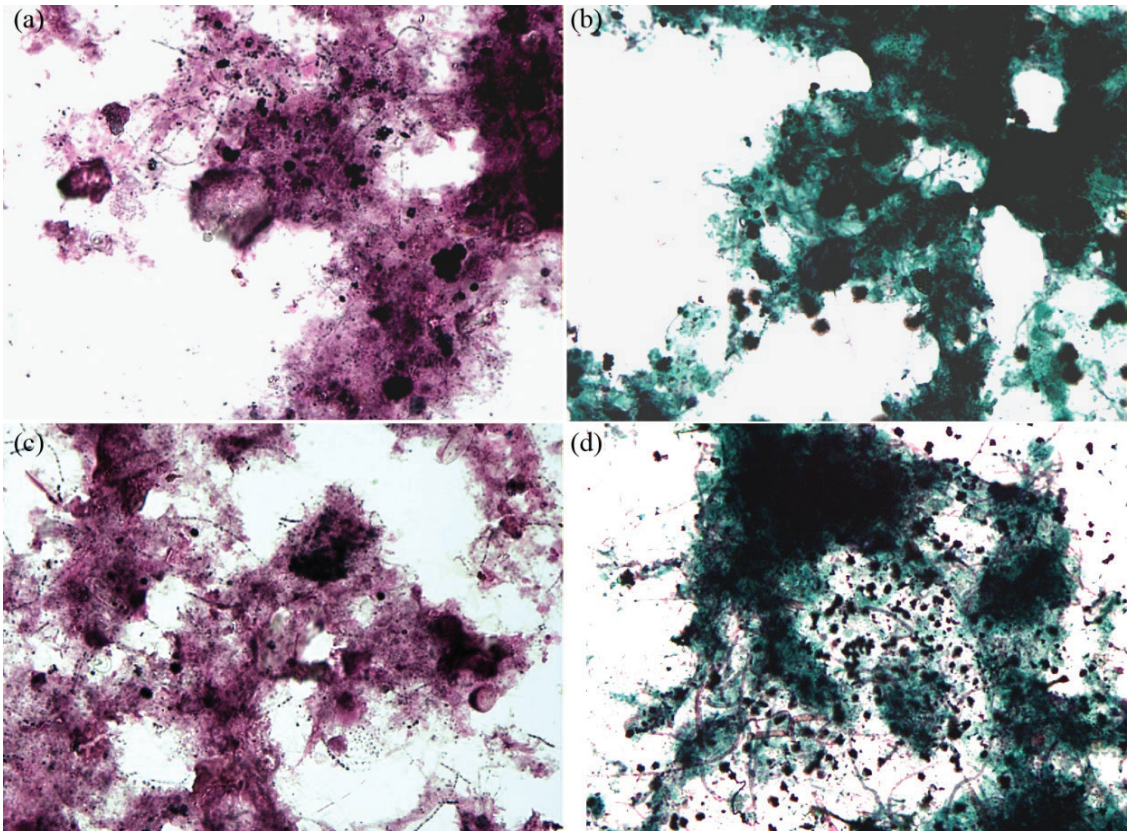

Fig. 7. Richness variation of PAOs on the biofilm in anaerobic (a), aerobic (b) of A^2O in-situ sludge reduction process and anaerobic (c), aerobic (d) of A^2O-SIC (scale 1:1,000).

biofilm are spherical and rod. Comparing Figs. 7(a) and (b), the number of bacilli and cocci containing black PHB particles on the biofilm was not changed after SIC running. But the number of filamentous bacteria increased. Comparing Figs. 7(c) and (d), the number of cocci containing black poly-P increased, and filamentous bacteria containing poly-P also appeared. Similar to the study of Zhang et al. [18], the content of filamentous bacteria increased gradually after SIC running. Filamentous bacteria were effectively adhered to micelles to form compact biofilm structures. In addition, cocci and bacilli can be connected to form filamentous bacteria. Studies show that the SIC system increased the organic load of aerobic tanks, contribute to the formation of biofilms and improve microbial activity.

3.5.2. Morphological analysis of microbial biofilms in the A²O-SIC process

Microbial morphology of biofilms was observed by SEM (Fig. 8). The microorganisms on the surface of the biofilm grow from the intensive and *Brevibacterium* in the front anaerobic to the bacterium with flocks of loose sludge in the anoxic, and the amount of sludge debris increased. In addition, the main structure of biofilm was loose sludge debris and bacillus filamentous bacteria connected in bundles, and surface depressed of the cocci in the aerobic area.

The influent water carries abundant organics into the anaerobic, in which had a higher microbial activity. Phosphorus released from phosphate-accumulating bacteria occurred in this region, and the dominant microorganism in the biofilm was rod-shaped phosphorus-accumulating bacteria. The abundant filamentous bacteria formed the lattice structure and adhered to microorganisms to form compact biofilm structure. The sludge debris induced by hydrolysis was observed in the anaerobic. The denitrification was mainly in the anoxic tank, and the dominant microorganism was bacillus denitrification, and it was clearly observed that the degree of microbial compaction at this stage was reduced. The aerobic area was mainly composed of fragmented sludge and long bacillus. The concentration of microorganisms in this area was further weakened, showing a porous structure.

The void structure can promote the material transfer inside and outside the biofilm, and the lack of carbon source may be the cause of sludge fragmentation due to the lack of carbon source resulting in the capture of dissolved cell release material as a supplementary carbon source by microorganisms in this area. Inadequate carbon sources caused microbes to capture dissolved cell-releasing substances as a supplementary carbon source inducing sludge fragmentation. The results of SEM showed that SIC could not inhibit microbial activity of biological process.

3.5.3. Microbial population analysis of the A²O-SIC

To further analyse the impact of SIC on the structure of the biological community, microbial population richness on the A²O-SIC biofilms is shown in Fig. 9. The diversity of

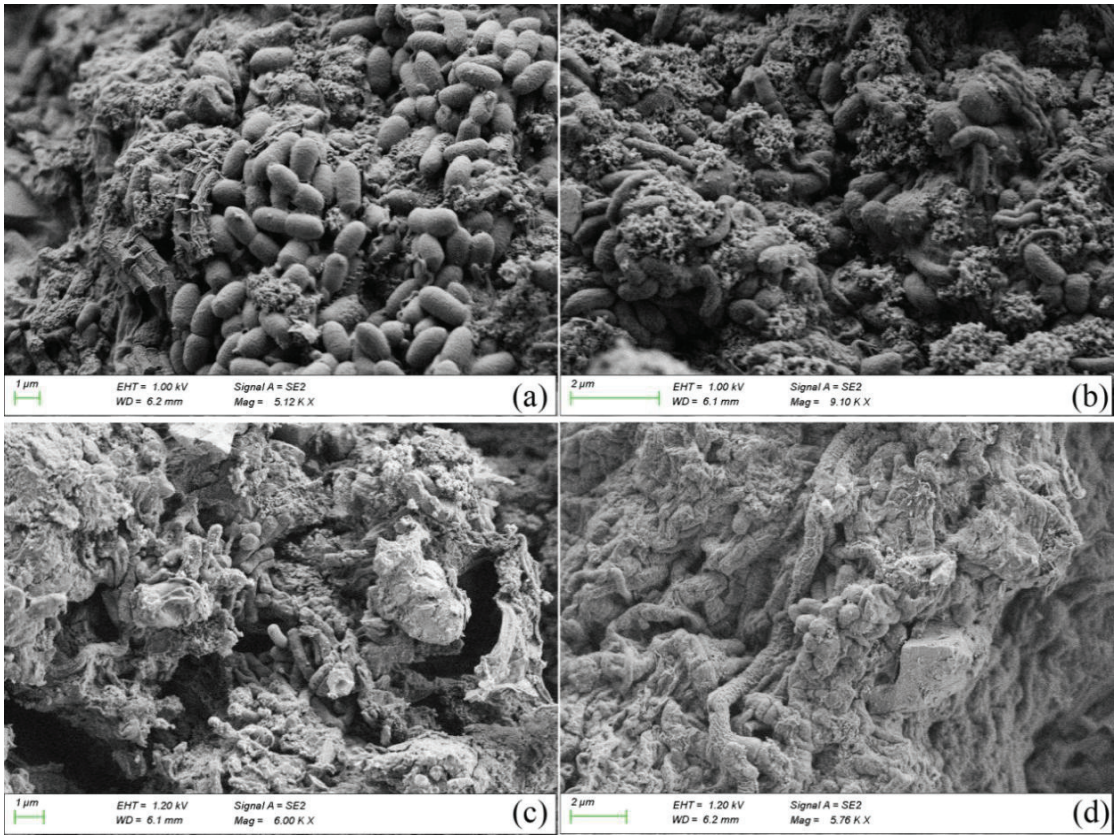

Fig. 8. Biofilm SEM image of A²O-SIC different area: (a) anaerobic, (b) anoxia, (c) middle of aerobic, and (d) end of aerobic area.

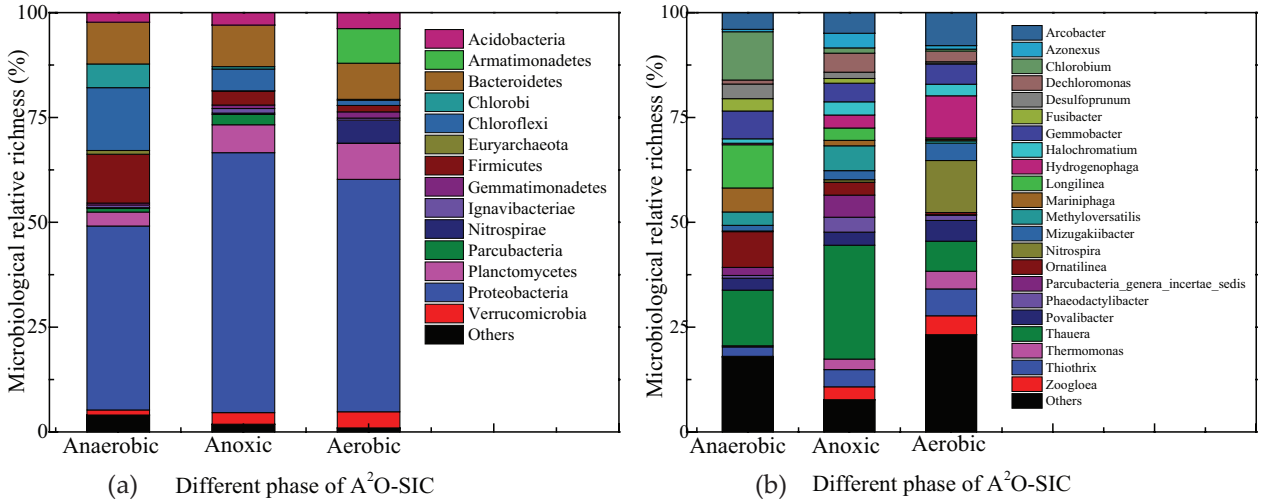

Fig. 9. Abundance of class (a) and genus (b) in anaerobic/anoxic/aerobic of A^{2}O-SIC.

microbial population on biofilm in anaerobic, anoxic, and aerobic was quite different. At the class level (Fig. 9(a)), the dominant microorganisms on the biofilm in the anaerobic are Proteobacteria (43.86%), Chloroflexi (14.98%) and Firmicutes (11.66%); these in anoxic were Proteobacteria (62.00%), Bacteroidetes (9.87%), and Planctomycetes (6.66%); and these in aerobic were *Proteobacteria* (55.43%), Bacteroidetes (8.62%), Planctomycetes (8.60%). Proteobacteria was dominant microorganism on biofilm in A^{2}O-SIC similar to the study of Dai et al. [29]. Similar to the study of traditional biological denitrification theory, Nitrospirae was enriched on biofilms in aerobic area [30].

Fig. 9(b) shows that the relative richness in genus level was quite different. The dominant microorganisms in the anaerobic were *Thauera* (14.33%), Chlorobium (12.44%), and *Longilinea* (11.13%); these in anoxic were *Thauera* (28.82%), *Methyloversatilis* (6.29%), and *Parcubacteria_genera_incertae_sedis* (5.59%); and these in aerobic were *Nitrospira* (12.80%), *Hydrogenophaga* (10.38%), and *Arcobacter* (7.86%). *Thauera* was a dominant microorganism in anaerobic and anoxic, and enriched in aerobic (14.33%, 28.82%, and 7.15%, respectively), indicating this genus associated with phosphorus removal and denitrification. Dai et al. [29] showed that *Thauera* can be found in denitrifying phosphorus removal sludge. This showed that the A^{2}O-SIC can promote simulation denitrification phosphorus removal using FSC. *Methyloversatilis*, related to phosphorus removal, was enriched on biofilms in anoxic and aerobic area, indicating that SIC running not affect biological phosphorus removal. The enrichment of *Nitrospira* on biofilms in aerobic area showed that nitrifying bacteria activity was not affected by SIC running in A^{2}O-SIC. *Hydrogenophaga*, related to denitrification reaction, enriched in aerobic tanks indicating that simultaneous nitrification and denitrification could be achieved in A^{2}O-SIC and improve denitrification effect. According to the microbial population analysis, A^{2}O-SIC is conducive to the growth of nitrifying bacteria *Nitrospira*, denitrifying microorganism *Hydrogenophaga*, and denitrifying phosphorus removal microorganism *Thauera*.

4. Conclusion

(1) This study showed that the A^{2}O in-situ sludge reduction and side-stream induced crystallization coupling system could achieve simultaneous high-efficiency sludge reduction and nitrogen and phosphorus removal. SIC can improve phosphorus removal simultaneous promote the enrichment of *Thauera, Methyloversatilis* in A^{2}O.

(2) The removal of A^{2}O-SIC was excellent. The phosphorus removal rate was 88.89% and the effluent phosphorus concentration was 0.54 mg·L^{-1}. The Y_{osb} of A^{2}O-SIC was 0.18±0.05 g MLSS/g COD, which effectively reduced excess sludge 18.18%.

(3) The focus of this study was to remove phosphorus by side-stream induced crystallization. SIC could promote the secretion of EPS in A^{2}O systems, improving coupling efficiency of the process. A^{2}O-SIC can recover the phosphorus resource (the product is HAP) in the sewage with reducing the sludge, which can provide an idea for comprehensive recovery of carbon and phosphorus resources from sewage.

Acknowledgments

This work was financially supported by the Natural Science Foundation of Shandong Province (ZR2016EEM32), the Doctoral Fund of Shandong Jianzhu University in 2015 (XNBS1511), the Scientific and technological Innovation Project of Planning and Design Institute of Huaihe River Basin Water Conservancy Administration Bureau of Shandong Province in 2018 (SFSJKY2018-01), and the National Natural Science Foundation (51878394), and the Science and Technology Plans of Ministry of Housing and Urban-Rural Development of the People's Republic of China, and Opening Projects of Beijing Advanced Innovation Center for Future Urban Design (UDC2017031612).

References

[1] H. Dai, X. Lu, Y. Peng, H. Zou, J. Shi, An efficient approach for phosphorus recovery from wastewater using series-coupled air-agitated crystallization reactors, Chemosphere, 165 (2016) 211–220.

[2] J. Keeley, A.D. Smith, S.J. Judd, P. Jarvis, Acidified and ultrafiltered recovered coagulants from water treatment works sludge for removal of phosphorus from wastewater, Water Res., 88 (2015) 380.
[3] Y.Z. Lu, H.F. Wang, T.A. Kotsopoulos, R.J. Zeng, Advanced phosphorus recovery using a novel SBR system with granular sludge in simultaneous nitrification, denitrification and phosphorus removal process, Appl. Microbiol. Biotechnol., 100 (2016) 4367–4374.
[4] H. Lee, Z. Yun, Comparison of biochemical characteristics between PAO and DPAO sludges, J. Environ. Sci. China, 26 (2014) 1340–1347.
[5] Y. Zhou, Ten Recommended Sludge Disposal Cases in China, The 2ndWater Industry Hotspot Forum Shanghai, 2010. Available at: http://news.solidwaste.com. cn/view/id_31404.
[6] Y. Wang, J. Li, W. Jia, N. Wang, H. Wang, S. Zhang, G. Chen, Enhanced nitrogen and phosphorus removal in the A^2/O process by hydrolysis and acidification of primary sludge, Desal. Wat. Treat., 52 (2014) 5144–5151.
[7] P. Yan, F. Ji, J. Wang, J. Fan, W. Guan, Q. Chen, Evaluation of sludge reduction and carbon source recovery from excess sludge by the advanced sludge reduction, inorganic solids separation, phosphorus recovery, and enhanced nutrient removal (SIPER) wastewater treatment process, Bioresour. Technol., 150 (2013) 344–351.
[8] P. Yan, J.S. Guo, J. Wang, Y.P. Chen, F.Y. Ji, Y. Dong, Enhanced nitrogen and phosphorus removal by an advanced simultaneous sludge reduction, inorganic solids separation, phosphorus recovery, and enhanced nutrient removal wastewater treatment process, Bioresour. Technol., 183 (2015) 181–187.
[9] Z. Yuan, S. Pratt, D.J. Batstone, Phosphorus recovery from wastewater through microbial processes, Curr. Opin. Biotechnol., 23 (2012) 878–883.
[10] G. Bertanza, R. Pedrazzani, L. Manili, L. Menoni, Bio-p release in the final clarifiers of a large wwtp with co-precipitation: key factors and troubleshooting, Chem. Eng. J., 230 (2013) 195–201.
[11] S.A. Parsons, J.A. Smith, Phosphorus removal and recovery from municipal wastewaters, Elements, 4 (2008) 109–112.
[12] T.P. Mokone, R.P. van Hille, A.E. Lewis, Metal sulphides from wastewater: assessing the impact of supersaturation control strategies, Water Res., 46 (2012) 2088–2100.
[13] W. Moerman, M. Carballa, A. Vandekerckhove, D. Derycke, W. Verstraete, Phosphate removal in agro-industry: pilot- and full-scale operational considerations of struvite crystallization, Water Res., 43 (2009) 1887–1892.
[14] G.J. Smolders, d.M.J. Van, M.C. van Loosdrecht, J.J. Heijnen, Model of the anaerobic metabolism of the biological phosphorus removal process: stoichiometry and pH influence, Biotechnol. Bioeng., 43 (1994) 461.
[15] H.L. Zhang, G.P. Sheng, W. Fang, Y.P. Wang, C.Y. Fang, L.M. Shao, H.Q. Yu, Calcium effect on the metabolic pathway of phosphorus accumulating organisms in enhanced biological phosphorus removal systems, Water Res., 84 (2015) 171.
[16] A. Ding, J. Wang, D. Lin, X. Tang, X. Cheng, H. Wang, L. Bai, G. Li, H. Liang, A low pressure gravity-driven membrane filtration (GDM) system for rainwater recycling: flux stabilization and removal performance, Chemosphere, 172 (2017) 21–28.
[17] S. Yang, P. Jin, X. Wang, Q. Zhang, X. Chen, Phosphate recovery through adsorption assisted precipitation using novel precipitation material developed from building waste: behavior and mechanism, Chem. Eng. J., 292 (2016) 246–254.
[18] S. Zhang, Q. Tian, M. Tang, F. Li, Effect of phosphorus recovery on phosphorous bioaccumulation/harvesting in an alternating anaerobic/aerobic biofilter system, Environ. Sci. China, 35 (2014) 979–986 (in Chinese).
[19] Y. Wang, B. Liu, K. Zhang, Y. Liu, X. Xu, J. Jia, Investigate of in situ sludge reduction in sequencing batch biofilm reactor: performances, mechanisms and comparison of different carriers, Front. Environ. Sci. Eng., 12 (2018) 5.
[20] W. Stumm, J.J. Morgan, Aquatic Chemistry: Chemical Equilibria and Rates in Natural waters, Cram101 Textbook Outlines to Accompany, 179 (1996) A277.
[21] M. Seckler, M. Danese, S. Derenzo, J.V. Valarelli, M. Giulietti, R. Rodríguezclemente, Influence of process conditions on hydroxyapatite crystallinity obtained by direct crystallization, Mater. Res., 2 (1999) 59–62.
[22] Y. Song, P.G. Weidler, U. Berg, R. Nüesch, D. Donnert, Calcite-seeded crystallization of calcium phosphate for phosphorus recovery, Chemosphere, 63 (2006) 236.
[23] T. Tervahauta, R.D.W. Van, R.L. Flemming, L.L. Hernández, G. Zeeman, C.J. Buisman, Calcium phosphate granulation in anaerobic treatment of black water: a new approach to phosphorus recovery, Water Res., 48 (2014) 632–642.
[24] C. Combes, C. Rey, Amorphous calcium phosphates: synthesis, properties and uses in biomaterials, Acta Biomater., 6 (2010) 3362–3378.
[25] Y. Zhang, F. Wang, X. Zhu, J. Zeng, Q. Zhao, X. Jiang, Extracellular polymeric substances govern the development of biofilm and mass transfer of polycyclic aromatic hydrocarbons for improved biodegradation, Bioresour. Technol., 193 (2015) 274.
[26] H. Zou, X. Lu, S. Abualhail, J. Shi, Q. Gu, Enrichment of PAO and DPAO responsible for phosphorus removal at low temperature, Environ. Prot. Eng., 40 (2014) 67–83.
[27] G.P. Sheng, J. Xu, W.H. Li, H.Q. Yu, Quantification of the interactions between Ca^{2+}, Hg^{2+}, and extracellular polymeric substances (eps) of sludge, Chemosphere, 93 (2013) 1436–1441.
[28] M. Wu, R. Zhu, H. Zhu, X. Dai, J. Yang, Phosphorus removal and simultaneous sludge reduction in humus soil sequencing batch reactor treating domestic wastewater, Chem. Eng. J., 215 (2013) 136–143.
[29] H. Dai, Z. Dai, L. Peng, Y. Wu, H. Zou, X. Lu, Metagenomic and metabolomic analysis reveals the effects of chemical phosphorus recovery on biological nutrient removal system, Chem. Eng. J., 328 (2017) 1087–1097.
[30] W.U. Xiao-Su, R.H. Liao, H.E. Gang, Integration of rapid separation biochemistry process and NAR exchange for treatment of rural sewage in suburbs of Beijing, China Water Wastewater, 2 (2014) 69–71 (In Chinese).

Supplementary information

1. Samples pretreatment for SEM

The samples were fixed 2.5% glutaraldehyde for 2 h at 4°C, and then they were rinsed in phosphate-buffered saline three times, and placed consecutively in vials containing 30%, 50%, 70%, 90%, and 100% ethanol for 15 min. Following dehydration, the samples were air-dried, attached onto viewing stages, and then sputter coated with gold to prevent static buildup during sample viewing. The samples were examined using SEM.

2. Specific operational steps of DNA extraction, PCR amplification and high-throughput 454 pyrosequencing

The three sludge samples collected from the biofilm of A^2O-SIC were combined for DNA extraction, which were used to reveal the effects of microbial community structures on sludge reduction. The 16s rRNA sequences were clustered into operational taxonomic units (OTUs) with an average length of 423 bp by setting a 3% distance limit (equivalent to 97% similarity) for anaerobic area sample (2,103 OTUs), anoxia area sample (2,419 OTUs) and aerobic area sample (2,072 OTUs). The theoretical maximum OTU values calculated using Chaol index, the species richness index theory, were 2,500.88 (anaerobic area), 3,044.33 (anoxic area), and 2,511.52 (aerobic area). The above values indicate that the species richness in different reaction regions in the A^2O-SIC was quite different, and the anoxic area population was the most abundant; the addition of SIC lateral flow units does not reduce the species richness of biological systems. The Shannon indexes for anaerobic, anoxia, and aerobic area samples were 5.71, 5.82, and 5.72, respectively. Higher richness and diversity in the microbial community can be represented by higher OTUs and Shannon diversity index indicated. Specific operational steps of DNA extraction, PCR amplification, and high-throughput 454 pyrosequencing were according to the Yang et al. [17].

3. Formulas of Y_{obs}

The formulas of accumulation and accumulation ratio of excess sludge values, and the detail of the formulas as following:

$$Y_{obs} = \frac{MLSS_e - MLSS_i + \sum_{i=1}^{n} MLSS_d}{(COD_i - COD_e) \times n} \quad \text{(S1)}$$

In this equation, Y_{obs} is the observed sludge yield (g MLSS·g^{-1} COD^{-1}); $MLSS_e$, and $MLSS_i$ are the concentration of MLSS (g·L^{-1}) on the 105th day and the first day, respectively; $MLSS_d$ is the accumulation of wasted sludge (g·L^{-1}) from the first day to the last day; COD_i and COD_e are the COD concentrations of the influent and effluent (g·L^{-1}); and n is the number of days in the experimental period.